A high-energy deposit in the Byzantine harbour of Yenikapı, Istanbul (Turkey)

Guénaëlle Bony [a],[*], Nick Marriner [a], Christophe Morhange [a], David Kaniewski [b], Doğan Perinçek [c]

[a] Université Aix-Marseille, Cerege UMR 6635, Centre Européen de Recherche et d'Enseignement des Géosciences de l'Environnement, Europôle Méditerranéen de l'Arbois, RD543/BP80, 13080 Aix en Provence, France
[b] Université de Toulouse, UMR 5245 CNRS - UPS, INPT, EcoLab (Laboratoire d'Ecologie Fonctionnelle), 118 route de Narbonne, 31062 Toulouse Cedex 9, France
[c] Çanakkale Onsekiz Mart University, Çanakkale, Turkey

ARTICLE INFO

Article history:
Available online xxx

ABSTRACT

A Byzantine harbour (Theodosian harbour) has been uncovered during excavations at Yenikapı, with a stratigraphic sequence spanning the past 7000 BP. In the marine part of the sedimentary sequence, a high-energy deposit has been interpreted as being of tsunami origin and related to the earthquake of 557 AD. This paper presents a bio-sedimentological analysis of this facies. The unit is characterised by coarse sands and gravels containing reworked material such as woods, bones, marble blocks, amphora fragments, ceramics, coins, shells and plant remains. The thickness of the facies varies between 10 and 100 cm. The sediment matrix is poorly sorted with skewness values indicative of a sub-tidal fine-sand environment. Many of the marine taxa have been reworked and diverse ecological assemblages are represented (lagoonal, coastal and open marine species). This unit is divided into three facies consistent with different phases of the tsunami drowning and water retreat. The basal facies corresponds to two tsunami wave trains, and the upper facies indicates the backwash flow.

© 2011 Elsevier Ltd and INQUA. All rights reserved.

1. Introduction

A Byzantine harbour (Theodosian harbour) has been uncovered during excavations at Yenikapı, headed by the Istanbul Archaeological Museum and the Marmaray Project (Kızıltan, 2007; Perinçek et al., 2007; Perinçek, 2008, 2010). The Marmaray project is centred around the construction of a metro station. The discovery of Theodosian harbour is of a great importance because 34 shipwrecks have been unearthed (Kocabaş and Özsait-Kocabaş, 2009), the first find of its scale and scope in an ancient harbour context. At the crossroads between Anatolia, southeastern Europe, the Black Sea and the Mediterranean, a palaeoenvironmental study of the harbour is crucial to understand the maritime history of the city.

The Theodosian harbour is located on the southwestern bank of Istanbul, presently ∼500 m from the coastline and infilled with alluvium from the Lycos River (Fig. 1). The ∼7 m sedimentary sequence observed in Theodosius' harbour consists of marine and fluvial facies. The stratigraphy attests to a number of environmental changes: (i) a continental marsh before the mid-Holocene marine transgression; (ii) a coastal environment that served as a harbour

between the 4th–11th centuries AD; and (iii) a final infill phase after the 11th century AD (Perinçek et al., 2007; Perinçek, 2008, 2010; Algan et al., 2009; Fig. 2).
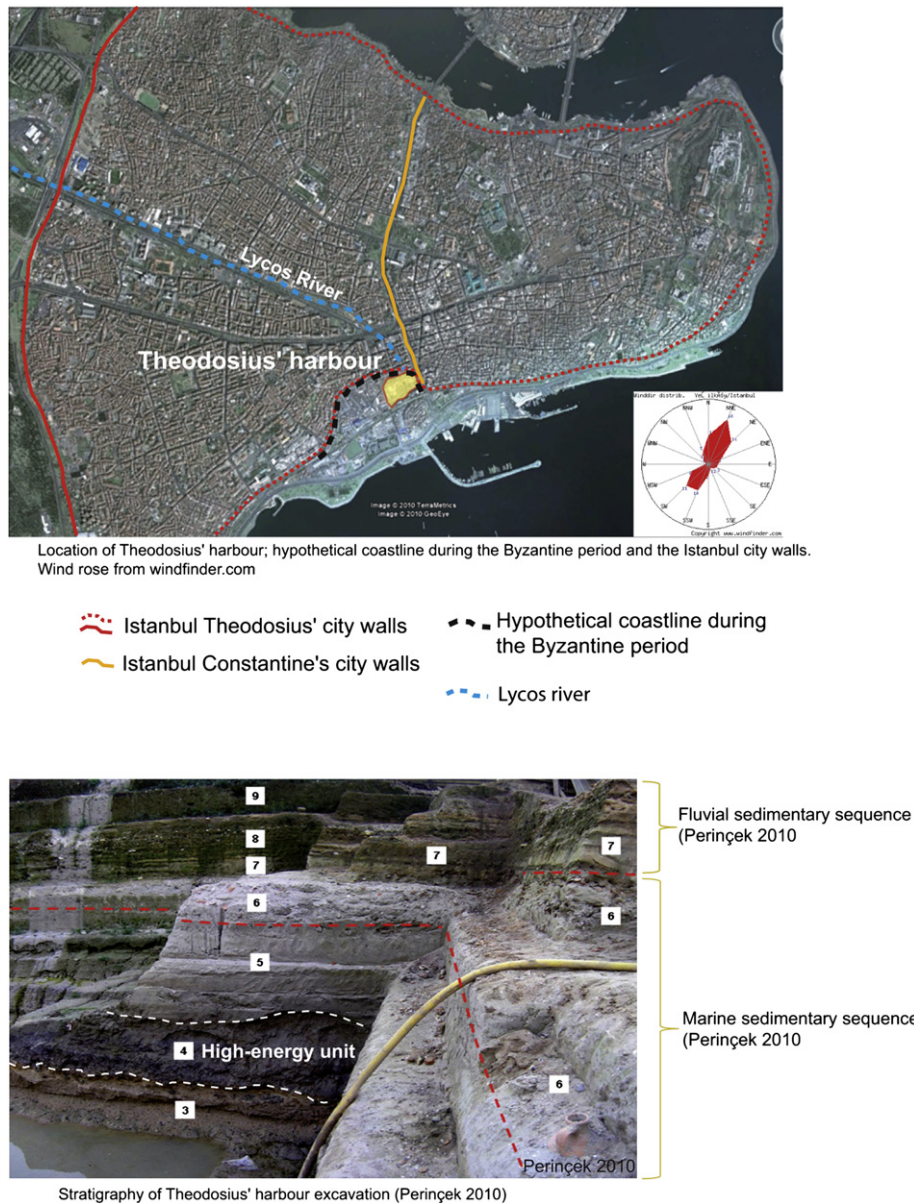
One of the marine units (unit 4) is characterised by (i) an irregular but sharp bottom contact and (ii) coarse-grained sediment (Figs. 3 and 4). This deposit is rich in reworked marine and continental material, including shells, coins, broken amphorae, ceramics, bones, skeleton and wooden fragments. Perinçek et al. (2007), Perinçek (2008, 2010), and Wazny et al. (2010), have interpreted the unit as a tsunamite linked to the 557 AD earthquake.

The Marmara region is a tectonically active belt of northwestern Turkey, characterised by the collision of the African and Eurasian plates. The North Anatolian Fault Zone (NAFZ) is one of the most active transform faults in the world (Perinçek, 1991; Yaltırak and Alpar, 2002; Brückner et al., 2010; Fig. 5) and has generated numerous earthquakes and tsunami throughout history (Fig. 5). For instance, ∼30 tsunami events have impacted the coasts of the Marmara Sea during the past 2000 years, and a numerical model of tsunami propagation in the Marmara predicts maximum near-shore tsunami heights of ∼6 m (Yalçıner et al., 2002). In comparison, the local wave climate of Istanbul is characterised by a maximum wave height of +2.5 m (Sağlam et al., 2010). The dominant wave direction is from the southwest to north-east.

The aim of this study is to understand the origin of this high-energy deposit (storm or tsunami generated?). Bio-sedimentological

* Corresponding author.
E-mail addresses: bony@cerege.fr (G. Bony), marriner@cerege.fr (N. Marriner), morhange@cerege.fr (C. Morhange), kaniewsk@cict.fr (D. Kaniewski), perincek@yahoo.com, perincek@comu.edu.tr (D. Perinçek).

Location of Theodosius' harbour; hypothetical coastline during the Byzantine period and the Istanbul city walls. Wind rose from windfinder.com

~~~~~ Istanbul Theodosius' city walls

—— Istanbul Constantine's city walls

• ▪ ▪ Hypothetical coastline during the Byzantine period

• ▪ ▪ Lycos river

Stratigraphy of Theodosius' harbour excavation (Perinçek 2010)

Fig. 1. Location of Theodosius' harbour. Historical and geomorphological settings. Stratigraphy of the Theodosius excavation.

tools were used to probe the stratigraphic signature of this high-energy event. Statistical analyses allow understanding of the wave energy linked to this event, and its impact inland.

2. Regional setting

2.1. Tectonic setting

Anatolia is surrounded by several seas (the Mediterranean, the Aegean, and the Black and Marmara Seas) where active tectonics occur (Hébert et al., 2005). This area is controlled by three main fault systems: the North Anatolian Fault (NAF), the East Anatolian Fault (EAF) and the Hellenic arc. The NAF is a major continental fault that is extruded westwards by the Anatolian block due to collision between the Arabian and Eurasian plates (Şengör et al., 1985; Yaltırak, 2002; Yalçıner et al., 2002; Hébert et al., 2005). Due to numerous earthquakes operating on the NAF, the fault is broken into two segments, west and east (Altınok et al., 2001a). The NAF is

characterised by horizontal ground displacements that do not usually generate tsunami. However, some of the earthquakes along the western segment of the fault have generated vertical ground movements leading to tsunami (Altınok et al., 2001a; Fig. 5). At least 90 major tsunami have impacted the Turkish coast in the past 3000 years and, between 120 AD and 1999 AD, ~30 tsunami occurred in the Marmara Sea (Altınok et al., 2001b; Yalçıner et al., 2002). A number of these tsunami impacted Istanbul, leading to considerable damage. For example, the 1509 AD earthquake generated a tsunami wave that spilt over the city walls and caused ~6-m wave run-up heights. The 1894 AD earthquake also inundated 200 m of land in Istanbul (Hébert et al., 2005).

2.2. Paleotsunami on the Istanbul coast in Byzantine times

The high-energy unit (unit 4), interpreted by Perinçek (2010) as a tsunami deposit, has been dated by ceramics found in the sediments. These chronological indicators date the event to between
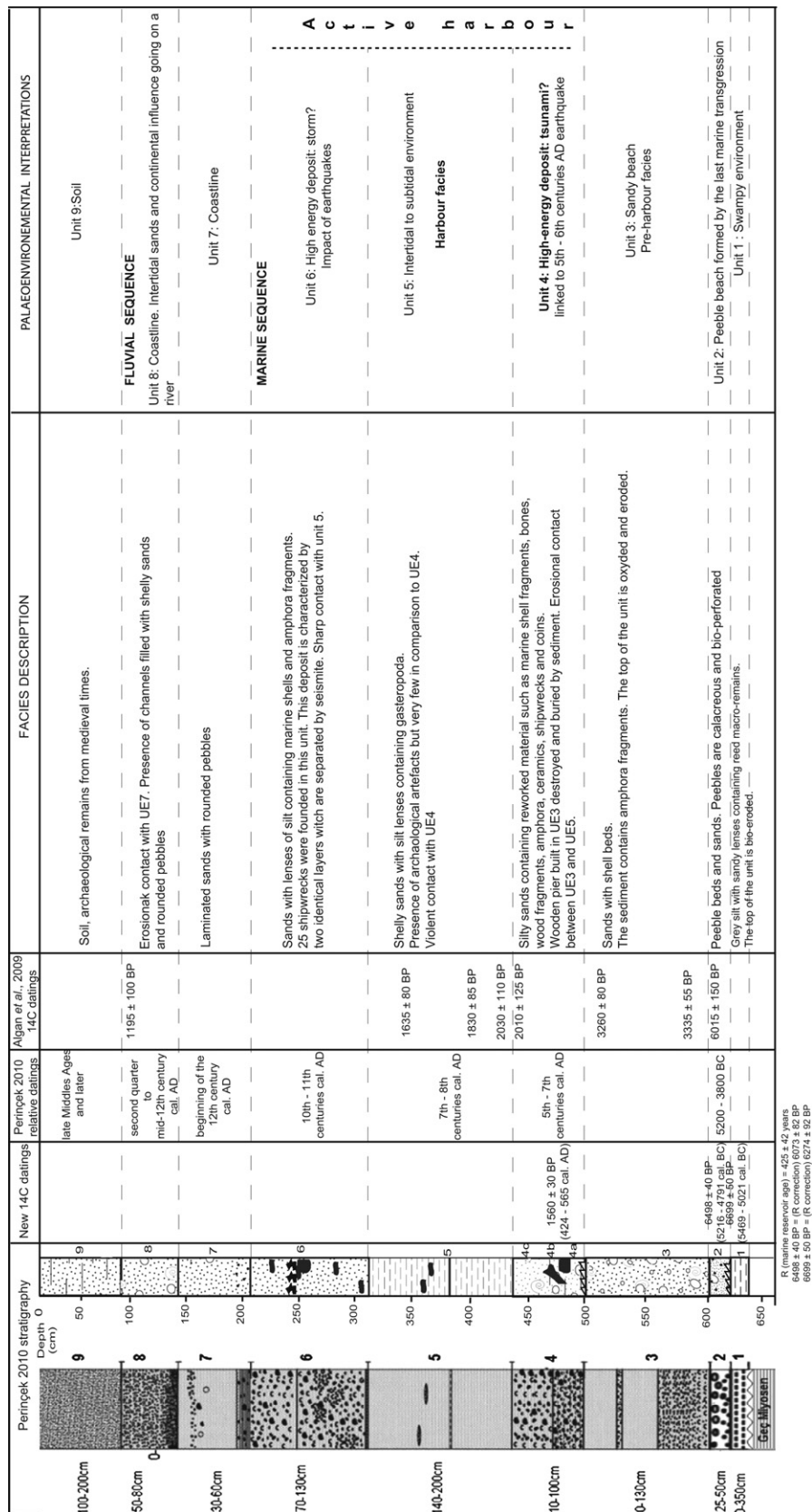
Fig. 2. Brief descriptions and interpretations of the excavation chronostratigraphy (adapted from Perinçek, 2010).
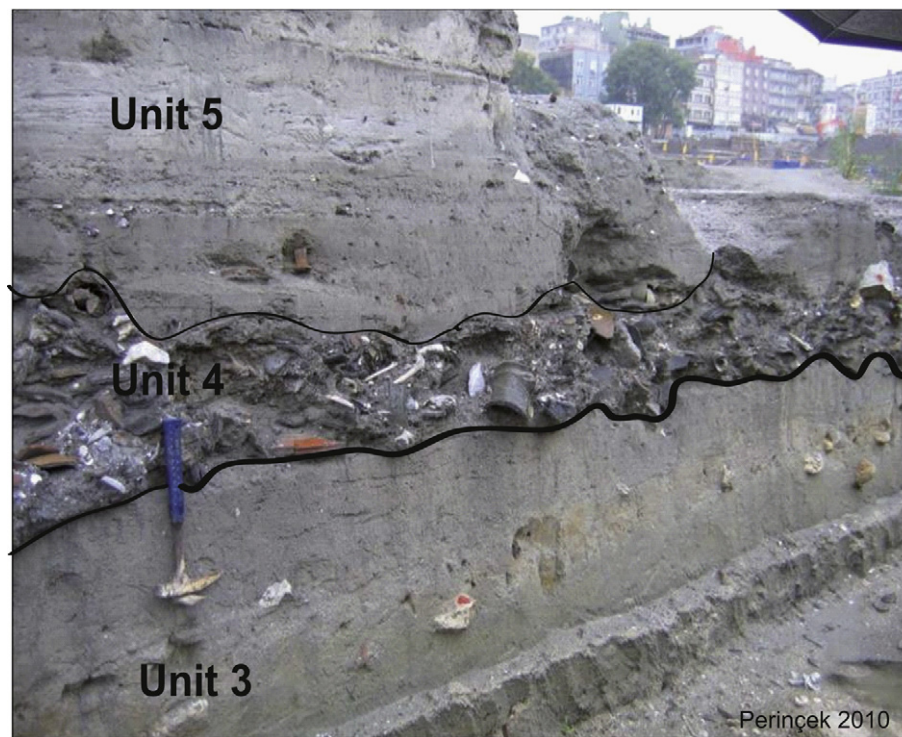
Fig. 3. Photograph of the high-energy unit (unit 4). Chaotic deposit containing coarse marine and terrestrial material, characterised by an erosional basal contact (Perinçek, 2010).
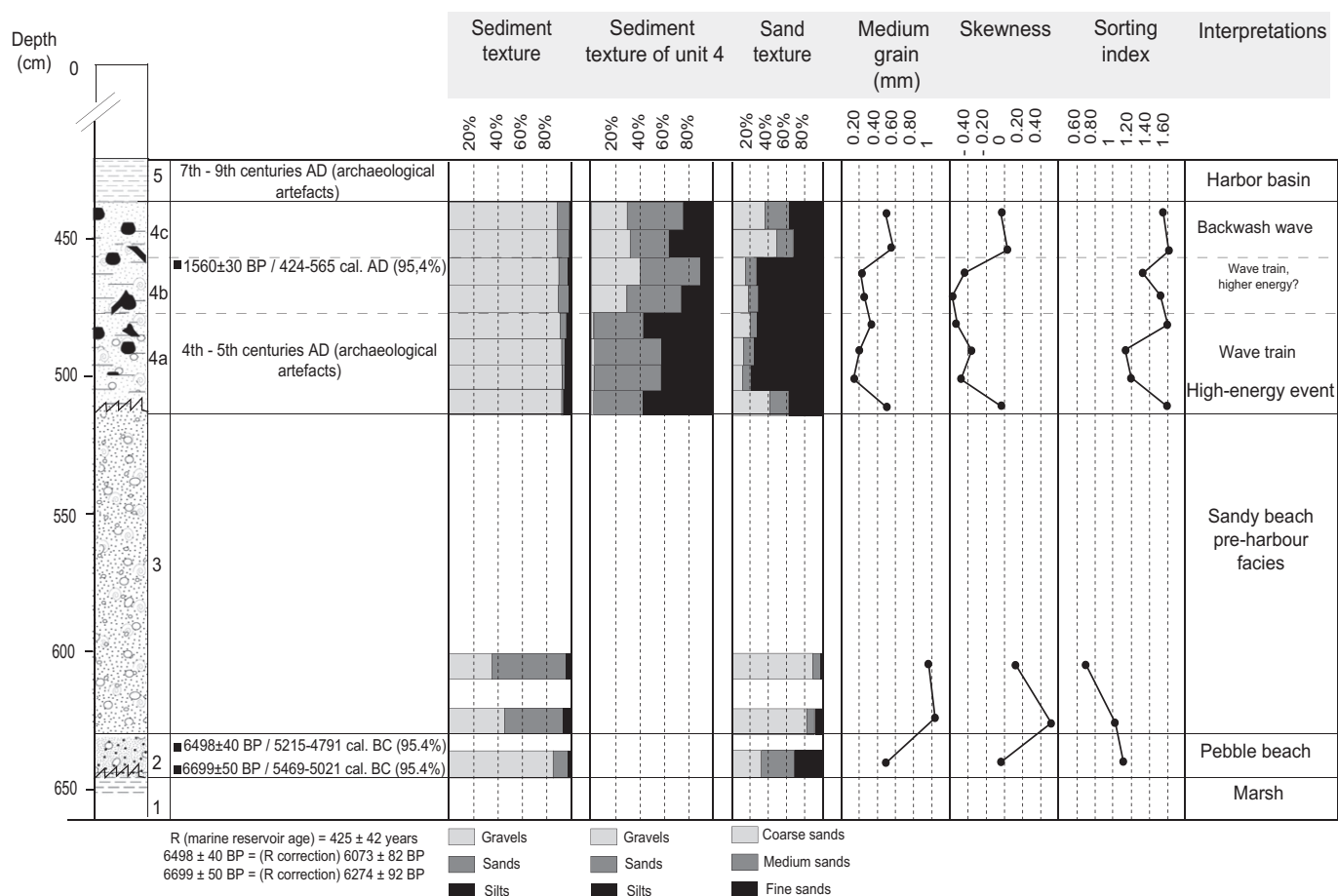

Fig. 4. Sedimentological log. Comparison of units 2, 3 and 4.

Seismotectonic map of the Sea of Marmara. The inset shows locations of tsunami events in and around the city of Istanbul. Numbers indicate the chronological order of tsunamis which occurred along the coasts of the Sea of Marmara between AD 120-1999 (Yalçiner et al., 2002).
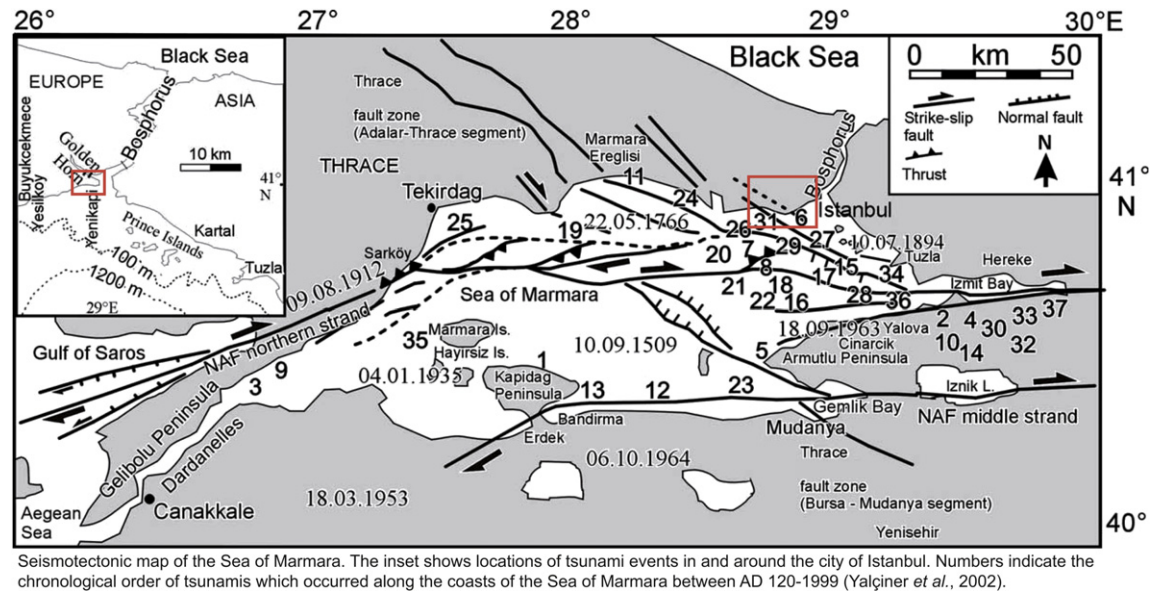
Fig. 5. Seismotectonic map of the Sea of Marmara (Yalçiner et al., 2002).

the 5th–7th centuries AD (Perinçek et al., 2007; Perinçek, 2008, 2010). During this period, five tsunami events impacted the Istanbul coast and are recorded in historical archives (Ambraseys, 1962, 2002, 2009; Antonopoulos, 1979; Soloviev, 1990; Guidoboni et al., 1994; Soloviev et al., 2000; Papadopoulos and Fokaefs, 2005): (1) January 447 AD, (2) September 477/480 AD, (3) August 553 AD, (4) December 557 AD, (5) 558 AD.

2.3. Historical setting

The coastal area of the Marmara Sea connects the Black Sea and the Aegean Sea through the straits of the Bosphorus and the Dardanelles. Since Antiquity, the region has been a pivotal area for maritime activity. Present-day Istanbul, the capital of the East Roman, Byzantium and Ottoman Empires, was an important centre of trade. During the Byzantine period, the city's commercial development necessitated the foundation of a new harbour. To meet this demand, the Theodosian harbour, protected by the city walls, was founded during the reign of Theodosius I (379–395), in a natural pocket beach at the mouth of the river Lycos (Fig. 1) and at the foot of the Seventh Hill. Under the reign of Theodosius II, a long jetty, oriented east-west, was built to shelter the basin. The harbour perimeter was more than 1600 m long and the jetty was 3.7 m wide. The harbour entrance was in the north-east (Grelois, 2007). Warehouses have been discovered at the eastern extremity of the harbour, indicating that Theodosius' harbour was a great commercial harbour (Müller-Wiener, 1998). The Theodosian harbour was used from the 4th century AD until at least the 11th century AD (Müller-Wiener, 1998; Algan et al., 2009; Kocabaş and Özsait-Kocabaş, 2009). It has been progressively infilled by

alluvium from the Lycos River. After the 12th century AD, the silted harbour basin was converted into the Langa gardens (Mundell-Mango, 2000; Mango, 2001).

3. Palaeoenvironmental setting and chronostratigraphy of the Holocene deposits

Theodosius harbour's transgressional-progradational sequence has been described and interpreted by Perinçek (2010) and Algan et al. (2009). An overview is given in Fig. 2. For a detailed discussion of these units, please see Perinçek (2010).

A marsh mud consistent with a swampy environment characterises unit 1. Unit 2 is coarse-grain sediment, consisting of pebbles and sands. The pebbles are bio-perforated and indicate calm marine sedimentation. Unit 2 was dated by Perinçek (2010) to 5200–3800 BC using archaeological artefacts; Algan et al. (2009) obtained an age of 6015 ± 150 BP (4840–4167 cal. BC; Paphia sp.). Radiocarbon dating obtained an age of 6498 ± 40 BP (5210–4840 cal. BC; Vermetus sp.). All these results are coherent and complementary. Unit 2 is a marine transgressive facies dated to ∼7000 cal. BP. Unit 3 is characterised by a shelly sandy texture and corresponds to a sandy beach environment. Unit 4, which is the focus of this paper, is a chaotic layer containing reworked marine and terrestrial material. This unit has been interpreted as a high-energy deposit by Algan et al. (2009), and more specifically as a tsunami layer by Perinçek (2010). Unit 5 is characterised by a shelly sand texture interfingered with silt layers. This sediment contains archaeological artefacts and is consistent with an ancient harbour unit (Theodosius' harbour) dated by Perinçek (2010) to the 7th–9th centuries AD. Unit 6 is characterised by a sandy texture

Table 1
Radiocarbon dates performed by the Poznan Radiocarbon Laboratory at Poznan.

Sample code	Sample name	Material	pMC	Err.	Age 14C (BP)	Err.	d13C	Err.	Calibrated age −95.4%
Poz-25849	Yenikapi U4 795 wood	Wood	82.34	0.3	1560	29	−27.3	0.5	424−565 cal. AD
Poz-25827	Yenikapi U4 795	Tellinidae	78.09	0.3	1985	30	−0.5	0.5	424−565 cal. AD
Poz-25824	Yenikapi U2 798	Vermetus sp.	44.53	0.23	6498	41	−3.9	0.5	5216−4791 cal. BC
Poz-25825	Yenikapi U2A 801	Vermetus sp.	43.43	0.24	6699	44	0.4	0.6	5469−5021 cal. BC

R(marine reservoir age) = 1560 − 1985 = 425 years σ = √(30 × 30 + 30 × 30) = 42 years Calibrate with Calib. Rev 6.0.1 with IntCal09 (Reimer et al., 2009).

with some silt lenses. These sediments contain amphorae fragments. Twenty-five shipwrecks have been found in this unit. Unit 6 has been interpreted as a storm deposit and dated to the 10th century AD (Perinçek, 2010). Unit 7 is characterised by sands and rounded pebbles, corresponding to a coastal area influenced by fluvial sediment inputs. Unit 8 is similar to unit 7 but with the palaeochannels infilled with sands and pebbles. Finally, unit 9 is consistent with a cultivated soil since 12th century AD.

4. Materials and methods

4.1. Sedimentology and radiocarbon chronology

Samples were collected from stratigraphic sections (Perinçek, 2008, 2010) during excavation. Unit 4 was sampled entirely, whereas the surrounding units (2 and 3) were only partially sampled. Grain-size analyses (~100 g of sediments) were undertaken to characterise sedimentary environments and sources. Units 2 and 4 have been radiocarbon dated and calibrated using Calib 6.0.1 with IntCal09 (Reimer et al., 2009). A wood fragment contained in unit 4 was used to date the high-energy event (Table 1). A marine shell (2 articulated valves of Tellinidae) found near the wood fragment was also dated and indicates a marine reservoir age of 425 ± 42 years. This is consistent with results obtained elsewhere, notably 415 ± 90 years for the Black Sea and Dardanelles strait (Siani et al., 2000, 2001). These dates closely match the international standard of 400 years used for Mediterranean coasts (Siani et al., 2001). Ceramics, also found in unit 4, have been identified to establish a historical chronology, indicating an age spanning the 5th–7th centuries AD (Perinçek et al., 2007; Perinçek, 2008, 2010).

4.2. Biostratigraphy

Bioindicators were extracted from ~3 g of sediments. The marine macrofauna (Péres and Picard, 1964; D'Angelo and Garguillo, 1978; Poppe and Goto, 2000a, b), ostracoda (Ruiz-Munoz et al., 1996; Guernet et al., 2003; Frenzel and Boomer, 2005; Cabral et al., 2006; Mischke et al., 2010) and foraminifera (Redois and Debenay, 1996; Kaminski et al., 2002; Duchemin and Jorissen, 2005; Murray, 2006) were identified using different reference books and papers. Fish bone remains were also identified (L. Villier and F. Rigoli, personal communication). Previous work has demonstrated that reworked faunal (foraminifera, ostracoda and molluscs) and botanical (charcoals, seeds) remains are good proxies for high-energy events (Leroy et al., 2002).

4.3. Statistical analyses

Multivariate statistical analyses were used to explore the biostratigraphical data. Neighbour Joining (NJ) analysis is an alternative method to hierarchical cluster analysis in multivariate data. In this study, NJ analysis is based on the presence/absence and abundance of taxa. NJ analysis was used to compute the lengths of tree branches, using branches as ecological distances between groups of taxa. NJ was computed using correlation as the similarity measure and final branch as the root.

The ordination of units has been tested using Non-Metric Multi-Dimensional Scaling (NMDS) and CABFAC factor analysis and Principal Coordinates (PC). Spearman's Rho was selected as the similarity measure in each analysis and the min span tree function was always used. This three-step statistical analysis is well adapted to detect potential gaps, discrepancies or discontinuities in the ordination of units. A major change in the data-set generates
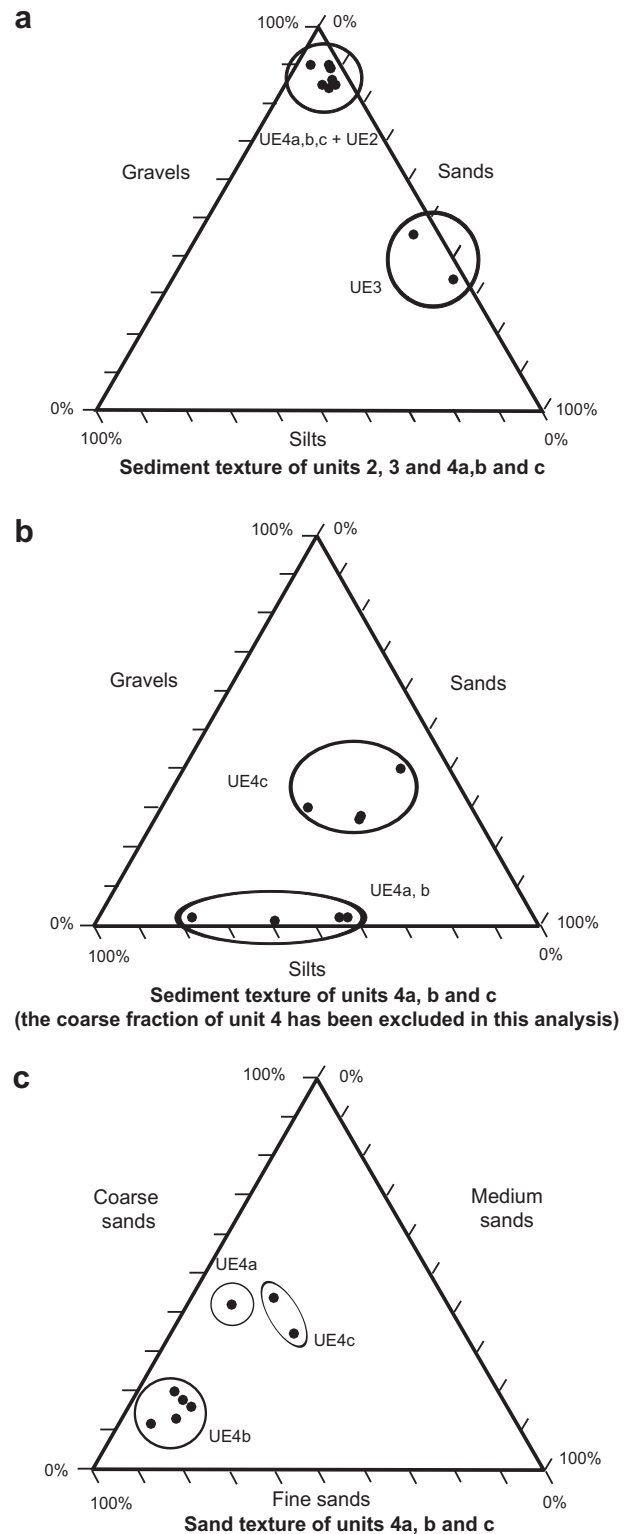
Fig. 6. Sediment texture of units 2, 3 and 4.

a break in the min span tree, causing the establishment of two different branches.

5. Results

The archaeological site of Yenikapı has recorded ~7000 years of sediment history. Fine-grained and coarse sediments respectively

indicate calm and exposed environments. Particular attention was paid to unit 4, which was interpreted by Perinçek (2008, 2010) as a high-energy event. Perinçek (2010) has dated this unit to the 5–7th centuries AD. Algan et al. (2009) have radiocarbon dated the top of this unit and obtained an age of 2010 ± 125 BP (645–95 cal. AD; *Cerastoderma edule*; Fig. 2). How can one explain this high-energy deposit in an artificially protected environment? For methodological reasons, this layer was compared and contrasted with two underlying units: the coarse basal layer (unit 2) and the pre-harbour sandy layer (unit 3).

5.1. Bio-sedimentological results

5.1.1. Unit 2: Holocene marine transgression

Unit 2 is characterised by a coarse texture (∼80% gravels; Figs. 4 and 6a) and a medium sand matrix (modal grain = 0.4 mm; Figs. 4 and 6b). The sorting index is positive and indicates poorly sorted sediment (Fig. 4). The gravels fraction comprises rounded and bio-perforated pebbles. *Vermetus triqueter* was observed in life position on these pebbles, indicating that they were in stationary position. Only the species *Anomia ephippium* is present, attesting to a coastal environment (Poppe and Goto, 2000a, b; D'Angelo and Garguillo, 1978; Figs. 7–10). Unit 2 has been dated to 6699 ± 50 BP and 6498 ± 40 BP (5463–5051 cal. BC, 5210–4840 cal. BC at 95.4%; *Vermetus* sp.; Table 1). According to Perinçek (2008, 2010) and Algan et al. (2009), this unit corresponds to a pebble beach formed by the Holocene marine transgression ∼7000 years ago.

5.1.2. Unit 3: pre-harbour sandy deposit

Unit 3, located between 6.3 and 5.15 m, is characterised by ∼35% biogenic gravels and a coarse sand matrix (modal grain = 1 mm; Figs. 4 and 6b). The skewness index is asymmetric

and the sorting index is positive. The sandy fraction (∼55%) is marine shell fragments. Macrofauna are present in significant quantities (60%) with, in contrast, low numbers of ostracoda and foraminifera (12% and 28%; Fig. 7). Coastal assemblages are dominant with ∼76% (Fig. 7) of species including *Bittium latreilli*, *Ammonia parkinsonia* and *Elphidium crispum* (Figs. 8–10). Lagoonal and marine species are present in low numbers (∼6% and 20%; Fig. 7), represented by *Scrobicularia plana* and *Cyprideis torosa* (Figs. 8–10). Such species mixing is typical of a pocket-beach environment (Marriner and Morhange, 2007).

5.1.3. Unit 4: high-energy event

This unit is located between ∼ 5.15 and 4.35 m (Figs. 3, 4 and 7–10). It is characterised by an irregular but sharp bottom contact with the underlying and overlying units (units 3 and 5; Figs. 3 and 4). This suggests that (i) the top of unit 3 was partially eroded by currents and (ii) unit 4 was deposited very abruptly. The thickness of the unit varies from 10 cm to 100 cm inside the harbour basin (Perinçek et al., 2007; Perinçek, 2008, 2010).

This unit corresponds to a chaotic deposit (Fig. 3). The gravel fraction dominates and comprises 80–100% of the total texture (Figs. 4 and 6a). Abundant reworked material of both continental and marine origin was observed, including trees, marble blocks, camel and horse bones, ceramics, coins and marine shell fragments. A wood sample yielded a radiocarbon age of 1560 ± 30 BP (424–565 cal. AD; wood; Table 1) and indicates that this unit was deposited during the Byzantine period, when the Theodosian harbour was operational. These relative and numerical chronological results are coherent (Algan et al., 2009; Perinçek, 2010; Stiros, 2010).

The matrix comprises ∼60% sand and ∼40% silt (Figs. 4 and 6b). The bottom of this unit is siltier than the top (∼40% versus ∼15%;
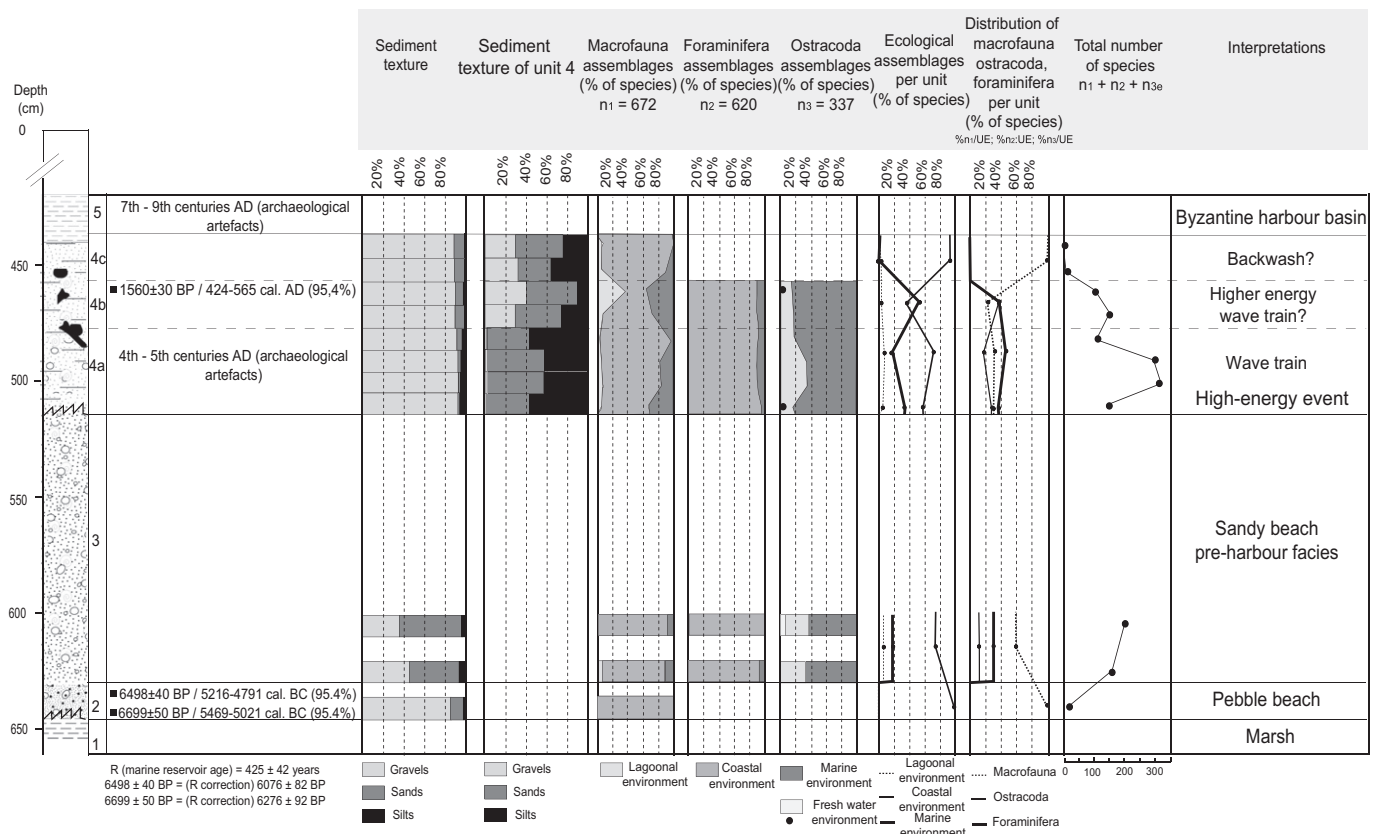

Fig. 7. Log of the biostratigraphical data. Comparison of the results for units 2, 3 and 4.
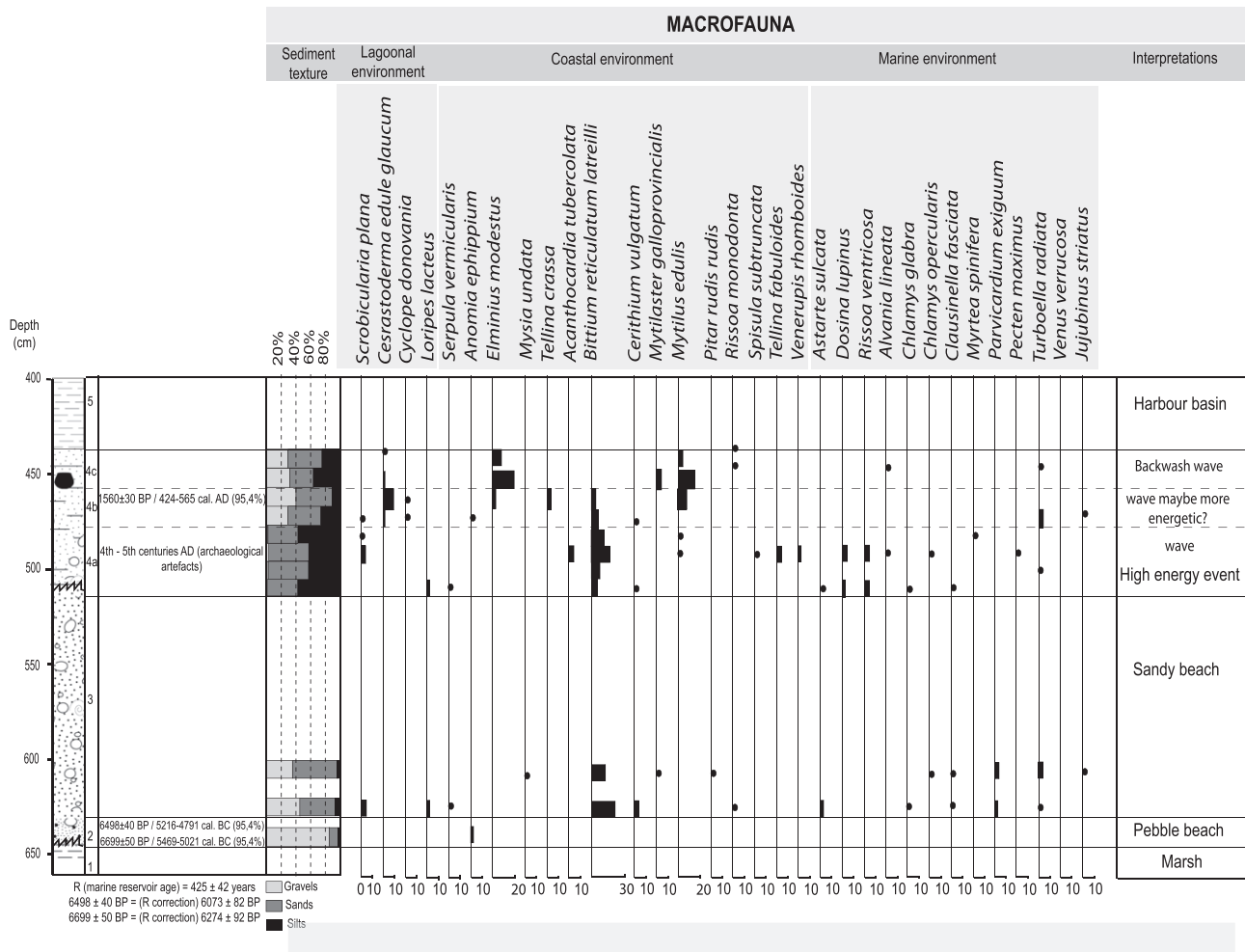
MACROFAUNA

Fig. 8. Detailed log of macrofauna.

Fig. 4). It is a clastic carbonate sediment made up of marine shell fragments, intact shells and ostracoda, attesting to a marine origin. The top of the unit comprises organic remains, charcoals, woods and seeds. The sediment is very poorly sorted (sorting index of ∼1.3; Fig. 4) indicating an abrupt event with no clear structure. The skewness index is negative, consistent with a "tail" of coarse sands (Folk and Ward, 1957). Based on grain-size analyses, unit 4 can be subdivided into three facies, 4a–c (Figs. 4, 6 and 7).
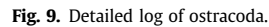
5.1.3.1. Unit 4a: up-rush facies 1. This facies, located at the base of unit 4, is characterised by a silty matrix composed of ∼60% silt and 40% sand, with a modal grain of 0.2 mm (Figs. 4 and 6b).

In this facies, there is a diversity of species assemblages similar to unit 3 (Fig. 7). The total number of species, notably foraminifera, is higher than in unit 3 (28% versus 46%). Coastal assemblages are dominant at 74% (Fig. 7) with species such as *B. latreilli, Triloculina* sp., *Ammonia* spp., *Elphidium* spp. and *Quinqueloculina* spp. (Bergin et al., 2006; Hussain et al., 2006; Figs. 8–10). The percentage of marine species is no greater than in unit 3 (18%), but the species diversity is higher. *Dosinia lupinus, Rissoa ventricosa, Alvania lineata, Myrtea spinifera, Pecten maximus* (for macrofauna) *Hiltermannicythere emaciata, Leptocythere* spp., *Loxoconcha tumida, Pseudocytherura calcarata, Callistocythere littoralis, Carinocythereis carinata, Costa edwardsii* (for ostracoda) and *Gavelinopsis praegeri, Milioninella subtrotunda, Nionella turgida* (for foraminifera) are new species in this facies (Nazik, 2001; Tunoglu, 2001; Bergin et al.,

2006; Ertekin and Tunoglu, 2008; Nachite et al., 2010; Figs. 8–10) and indicate significant marine input. High relative abundances of offshore microfauna such as *Semicytherura* spp., *Pseudocytherura* spp., *Xestoleberis* spp., *Urocythereis* spp., *Bulmina* spp. and *Nionella* spp. (Kaminski et al., 2002; Cabral et al., 2006) is unusual because their fragile tests are usually broken by high-energy waves. Their presence indicates a sudden opening of the depositional environment (Nanayama and Shigeno, 2006; Dawson and Stewart, 2007a). It is suggested that facies 4a corresponds to the first tsunami wave train deposit.

5.1.3.2. Unit 4b: up-rush facies 2. This second facies is characterised by a sandy matrix (∼60%; Figs. 4 and 6b) with a modal grain of ∼0.3 mm. In this facies, species assemblages are also juxtaposed. The major difference with facies 4a is that marine species are dominant (58% versus 18% for facies 4a; Fig. 7) including taxa such as *Loxoconcha rhomboidea, L. tumida, Loxoconcha agilis* and *Xestoleberis dispar* (Nazik, 2001; Bergin et al., 2006; Ertekin and Tunoglu, 2008; Nachite et al., 2010; Figs. 8–10). The percentage of lagoonal species decreases slightly (5% versus 8%) whereas the percentage of marine species increases (58% versus 18%) consistent with a more important marine input (Figs. 8–10). Foraminifera and ostracoda are present in similar relative abundances (38%). As for facies 4a, the microfauna attest to significant marine input. A sharp increase in the relative abundance of marine species indicates that the wave train was possibly more energetic than that of facies 4a. It has been

Fig. 9. Detailed log of ostracoda.

suggested that the major wave in tsunami events is not commonly the first wave train (H. Hébert, personal communication).

5.1.3.3. Unit 4c: backwash facies. This facies is characterised by a sandy matrix (~40%), comprising ~40% coarse sands with a modal grain of 0.6 mm (Figs. 4 and 6b). The sediment is rich in charcoals, seeds, plant remains and ceramic fragments of continental origin. For the biostratigraphy, the total number of species decreases suddenly. Molluscs are dominated by the coastal assemblage; ostracoda and foraminifera are absent (Figs. 7–10). *Elminus modestus*, *Mytilus edulis* and *Mytilaster galloprovincialis* are present. These species are common on wooden piers in harbour basins (Watson et al., 2005). The absence of microfauna is linked to continental sediment inputs into the harbour. These data are consistent with backwash currents reworking a poorly sorted mixture of soil, non-marine sands and plant fragments (Nanayama et al., 2000). This unit is interpreted as a tsunami backwash facies.

5.2. Statistical analyses

NJ analysis was used to explore the biostratigraphical data (Fig. 11a,b). The ordination of species is computed using the total variance of each species from the different units. This numerical-based classification allows definition of statistically significant assemblages. A first classification of species was established for all units (Fig. 11a). This analysis strengthens the bio-sedimentological data, because the ordination of species shows a mixing of assemblages indicative of an estuarine environment. Units 2 and 3, which

were compared to unit 4, correspond to coastal environments characterised by mixing species. This first result confirms the palaeoenvironmental interpretation. The second NJ was performed exclusively on unit 4, and shows a mixing of taxa but with a dominance of marine assemblages, indicative of significant marine input (Fig. 11b) which is coherent and confirms these results.

The numerical model was established using three methods: MNDS, CABFAC, and PC. These three tests are useful in quantifying the mathematical links or discontinuities between sedimentary units, using the biostratigraphy and grain-size data as the initial matrix. Units 2 and 3 (Fig. 12) show a continuous and unbroken tree span, suggesting no major shift in the raw data. The maximum discontinuity recorded corresponds to unit 4b, which is clearly differentiated from the underlying units, suggesting high variation in the original matrix. This confirms the biological results interpreting facies 4b as a more energetic wave train. The three ordinations also show that unit 4a is discontinuous but similar to unit 3. This first facies (4a) is characterised by reworking sediment of unit 3. This statistical approach has allowed confirmation of the interpretations.

6. Discussion: tsunami versus storm deposit

6.1. Bio-sedimentological arguments for a tsunami deposit

Tsunami and storms are two phenomena that set marine water in motion. Although both result from different forcing agents, they cause coastal flooding with high overland flow velocities. In many
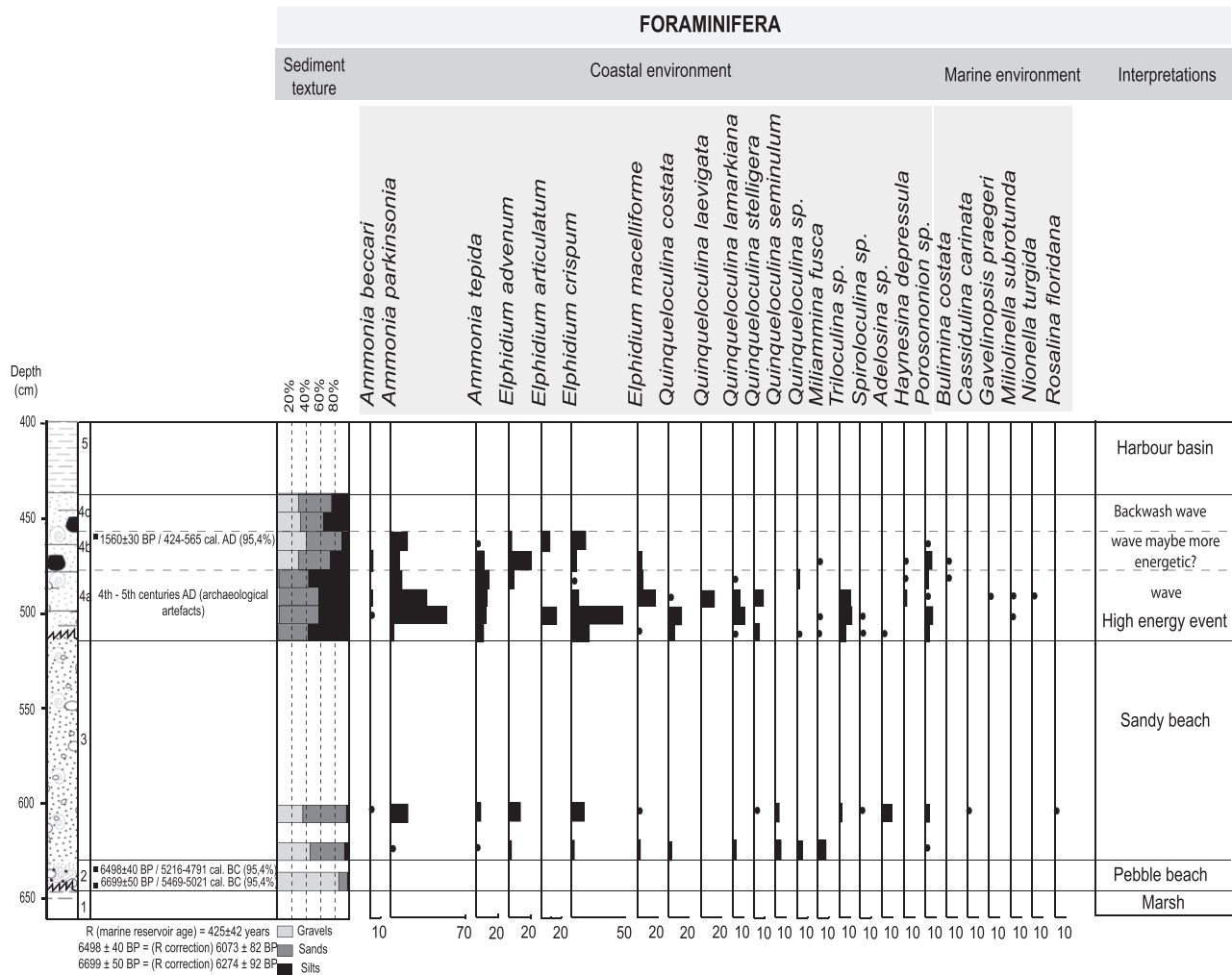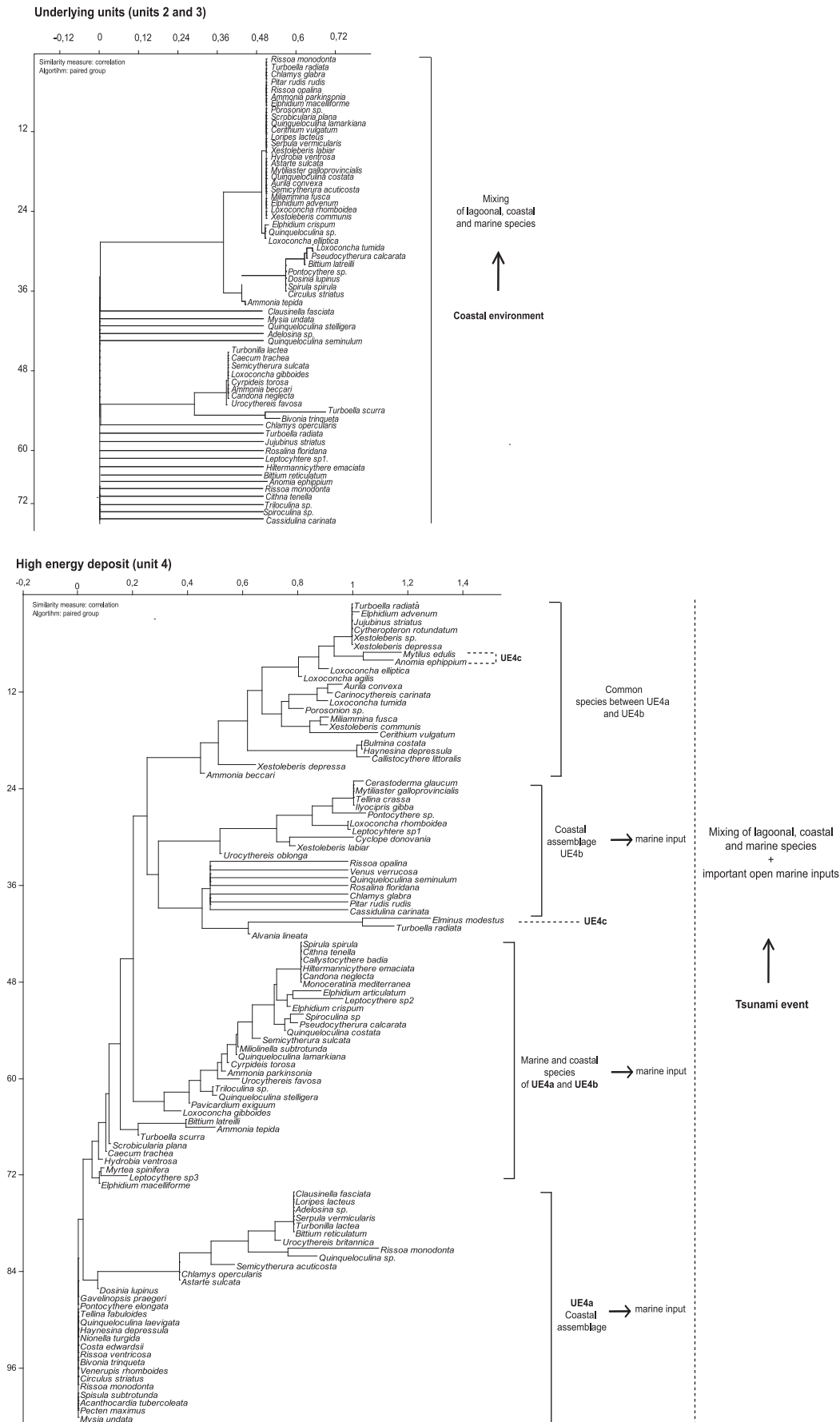
Fig. 10. Detailed log of foraminifera.

cases, their sedimentological signatures are similar and therefore difficult to differentiate unequivocally (Foster et al., 1991; Shanmugan, 2006; Morton et al., 2007). Some publications have addressed this subject in detail, establishing a series of criteria to distinguish between storm and tsunami deposits (Dawson and Shi, 2000; Tuttle et al., 2004; Goff et al., 2004; Kortekaas and Dawson, 2007; Morton et al., 2007). A number of criteria help to link unit 4 with a tsunami event.

Unit 4 is characterised by a

(1) lower erosional contact. This irregular contact indicates erosion by currents typical of water retreat before the tsunami up-rush (Fujiwara et al., 2000; Goff et al., 2004; Hawkes et al., 2007; Morton et al., 2007).

(2) This coarse and chaotic unit is present across the excavation site. Tsunami deposits are characterised by a continuous layer, whereas storm deposits are characterised by patchy sedimentation (Dawson and Stewart, 2007b).

(3) A sedimentological aberration is present. The coarse destruction unit of marine and terrestrial origin has been deposited inside a protected harbour. This stratigraphy is atypical of an artificially protected environment (Marriner and Morhange, 2007).

(4) The presence of different facies inside the high-energy deposit is an argument for a tsunami deposit. These facies indicate two different energy levels correlated with a tsunami waves train,

differentiating between a run-up facies and a backwash facies. According to Nanayama et al. (2000), Goff et al. (2004), Smith et al. (2004), Hawkes et al. (2007), Dawson and Stewart (2007a), Morton et al. (2007), Bruins et al. (2008), the wave train generates around two or three sedimentary layers. There is generally a clear distinction between tsunami run-up waves and the backwash waves, which is consistent with the data (Wassmer et al., 2007). In general, storm deposits are more stratified. Moreover, the presence of the backwash facies is coherent with a tsunami. The inundation causes upslope erosion, reworking terrestrial material such as wood, seeds and organic mud.

(5) The presence of marine species such as *S. plana, Mytilaster galloprovincalis*, *Pontocythere* spp., *Loxoconcha* spp., *Urocythereis* spp., *Rossalina* spp., *Cassidulina* spp. and *Bulmina* spp. indicate reworking from offshore. The reworking of marine, coastal and lagoonal species is typical of tsunami deposits (Fujiwara et al., 2000; Hussain et al., 2006; Morales et al., 2008; Mamo et al., 2009; Ruiz et al., 2009; Vött et al., 2009). The absence of deep-sea foraminifera can be linked to the coastal bathymetry and shallow coastal seafloor. In front of Istanbul, the shelf is relatively wide, ~12 km, with a water depth of ~200 m (Hébert et al., 2005; C. Grall, personal communication).

(6) The morphoscopy of macrofauna is characterised by broken shells and angular fragments. The presence of this type of

Fig. 11. Neighbour joining results for the high-energy unit 4 and for the underlying units (units 2 and 3).
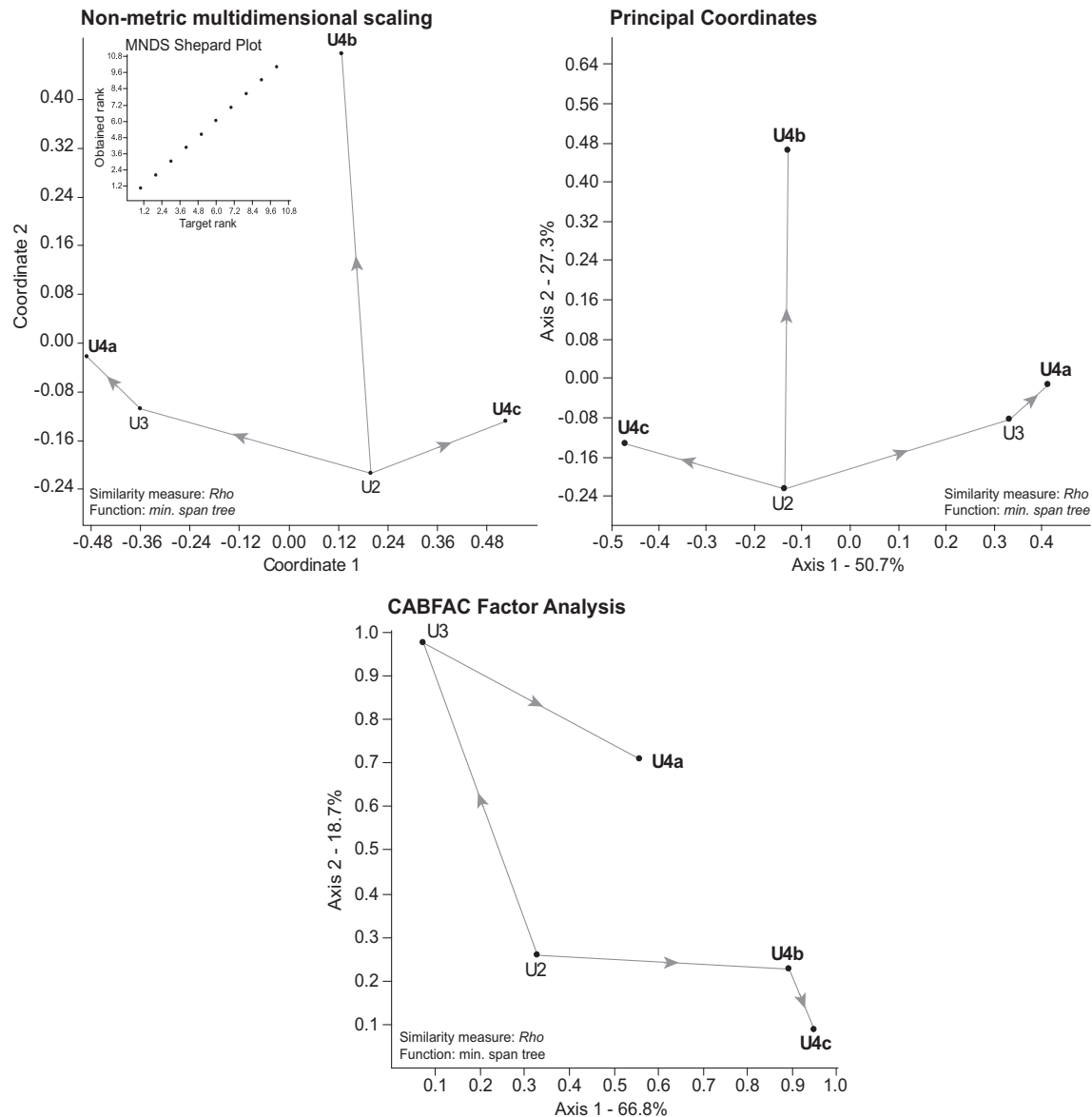
Fig. 12. Statistical results of the three tests: non-metric multi-dimensional scaling (NMDS) CABFAC factor analysis (CABFAC) and Principal coordinates (PC).

macrofauna within the harbour basin indicates high-energy processes (Dawson and Shi, 2000; Donato et al., 2008).

6.2. Geomorphological and historical evidence for tsunami events

Protected harbour basins, such as the Theodosian harbour, are generally good archives for this type of deposit because they act as sediment traps (Marriner and Morhange, 2007). In the case of Istanbul and the Marmara Sea, it is well documented that the Western North Anatolian Fault (WNAF) is an active fault that has triggered numerous tsunami, including the recent Izmit tsunami in 1999 with a magnitude of $M_w = 7.4$ (Tinti et al., 2006). The WNAF lies at $90°$ to the Istanbul coast and explains why Istanbul is particularly prone to tsunami (Ward, 2002).

During the Byzantine period, five tsunami events are correlated with the radiocarbon (1560 ± 30 BP; 424–565 cal. AD at 95.4%; Table 1) and archaeological (5th–7th century AD) data obtained for unit 4. These include the tsunami of: (i) 447 AD, (ii) 477–480 AD, (iii) 553 AD, (iv) 557 AD, and (v) 558 AD. According to Guidoboni

et al. (1994), the tsunami of 447 AD impacted Istanbul with extreme violence: "…Evagrius considers the earthquake to have been one of the major disasters of the reign of Theodosius II" (Evagrius, 1.17 in Guidoboni et al., 1994), and Malalas specifies that "It happened late in the evening, and the city was razed to the ground and flooded by the sea" (Malalas, 363, 4 in Guidoboni et al., 1994). Between 477 and 480 AD, an earthquake impacted the coast of the Marmara Sea and is recorded in historical archives from Istanbul (Guidoboni et al., 1994). According to Soloviev et al. (2000), the 558 AD tsunami was felt throughout the Bosphorus strait.

One event has been recorded in the stratigraphy of the Theodosian harbour. Of the five tsunami, only one had sufficient energy to allow sedimentation inside the protected harbour basin. Dawson and Stewart (2007a) have highlighted the importance of energy thresholds in tsunami preservation in the geological record. Tsunami wave amplitude is therefore related to earthquake magnitude.

Perinçek et al., (2007) and Perinçek (2008, 2010) favour the tsunami of 557 AD because the earthquake was particularly violent, although the 447 AD tsunami could also be the origin of the chaotic

sedimentation inside the harbour. First, the 557 AD event is widely attested in all tsunami catalogues. Ancient historians such as Marcellinus and Malalas describe the seismic wave: "... innumerable calamities happened both by land and sea ... (Marcellinus, Com 92.6-10 in Guidoboni et al., 1994). The sea also cast up dead fish; many islands were submerged, and ships were stranded by the retreat of the waters ....". The tsunami of 477 is also described by Malalas: "... the sea became very wild, rushed right in, engulfed a part of what had formerly been land, and destroyed several houses ..." (Malalas, 385 in Guidoboni et al., 1994). Because of the dating uncertainties (424–565 cal. AD at 95, 4%), it is difficult to attribute the high-energy facies to one particular event. Using dendrochronology, P. I. Kuniholm (pers. comm. 14/04/11) has shown that unit four is dated to 588 AD or a very few years later. In light of this, there appears to be no connection between the high-energy deposit and the 557 AD earthquake. A further problem is the absence of preservation of the other four tsunami deposits. Amnesia is the rule and archiving is the exception!

7. Conclusion

This study focused on the bio-sedimentological analysis of a high-energy deposit to explore its origin (storm or tsunami?). The sedimentological results indicate a coarse facies with a poorly sorted sand matrix. The unconformable basal contact shows erosion during pre-tsunami water retreat, and the subsequent uprush. Bioindicators present a mixing of stocks, which allow differentiation of different wave trains. The second wave train could have had higher energy levels. At the top of the unit, the presence of reworked terrestrial material is attributed to the backwash waves train. The use of statistical methods in this study is novel, and adds to the robustness of the conclusions.

In conclusion, this study demonstrates that the Theodosian harbour was impacted by at least one tsunami event during the Byzantine period. The bio-sedimentological, geomorphological evidences and historical records constitute sound arguments for this high-energy event. Investigation of the deposit in an archaeological context has allowed comparison of radiocarbon dates with archaeological chronologies. The study highlights the importance of marine inputs following a high-magnitude earthquake. This multidisciplinary study provides a framework to understand the bio-sedimentological signature of tsunami events in the wider Mediterranean in ancient harbour contexts (Morhange and Marriner, 2010).

References

Algan, O., Namık Yalçın, M., Özdoğan, M., Yılmaz, I., Sarı, E., Kırcı-Elmas, E., Ongan, D., Bulkan-Yesıladalı, Ö, Yılmaz, Y., Karamut, I., 2009. A short note on the geo-archaeological significance of the ancient Theodosius harbour (Istanbul, Turkey). Quaternary Research 72, 457–461.

Altınok, Y., Tinti, S., Alpar, B., Yalçıner, A.C., Ersoy, S., Bortolucci, E., Armigliato, A., 2001a. The tsunami of August 17, 1999 in Izmit bay, Turkey. Natural Hazards 24, 133–146.

Altınok, Y., Ersoy, S., Yalçıner, A.C., Alpar, B., Kuran, U., 2001b. Historical tsunami in the Sea of Marmara. ITS 2001 proceedings, Session 4, Number 4–2, 527–534.

Ambraseys, N., 1962. Data for the investigation of the seismic sea-waves in the Eastern Mediterranean. Bulletin of Seismological Society of America 52 (4), 895–913.

Ambraseys, N., 2002. The seismic activity of the Marmara Sea region over the last 2000 years. Bulletin of Seismological Society of America 92 (1), 1–18.

Ambraseys, N., 2009. Earthquakes in the Mediterranean and Middle East: A Multidisciplinary Study of Seismicity up to 1900. Cambridge University Press. 947.

Antonopoulos, J., 1979. Catalogue of tsunami in the eastern Mediterranean from Antiquity to present Times. Annali di geofisica 32, 113–130.

Bergin, F., Kucuksezgin, F., Uluturhan, E., Barut, I.F., Meric, E., Avsar, N., Nazik, A., 2006. The response of benthic foraminifera and ostracoda to heavy metal pollution in Gulf of Izmir (Eastern Aegean Sea). Estuarine, Coastal and Shelf Science 66, 368–386.

Brückner, H., Kelterbaum, B., Marunchak, O., Porotov, A., Vött, A., 2010. The Holocene sea level story since 7500 BP – Lessons from the eastern Mediterranean, the Black and the Azov seas. Quaternary International 225, 160–179.

Bruins, H.J., MacGillivray, J.A., Synolakis, C.E., Benjamini, C., Keller, J., Kisch, H.J., Klügel, A., Van der Plicht, J., 2008. Geoarchaeological tsunami deposits at palaikastro (Crete) and the late Minoan IE eruption of Santorini. Journal of Archaeological Science 35, 191–212.

Cabral, M.C., Freitas, M.C., Andrade, C., Cruces, A., 2006. Coastal evolution and Holocene ostracods in Melides lagoon (SW Portugal). Marine Micropaleontology 60, 181–204.

D'Angelo, G., Garguillo, S., 1978. Guida alle conchiglie mediterranee. Fabbri Milano. 216.

Dawson, A.G., Shi, S., 2000. Tsunami deposits. Pure and Applied Geophysics 157, 875–897.

Dawson, A.G., Stewart, I., 2007a. Tsunami deposits in the geological record. Sedimentary Geology 200, 166–183.

Dawson, A.G., Stewart, I., 2007b. Tsunami Geoscience. Progress in Physical Geography 31, 575–590.

Donato, S.V., Reinhardt, E.G., Boyce, J.I., Rothaus, R., Vosmer, T., 2008. Identifying tsunami deposits using bivalve shell taphonomy. Geology 36, 199–202.

Duchemin, G., Jorissen, F.J., 2005. Living benthic foraminifera from "la grande vasière" French Atlantic continental shelf, faunal composition and microhabitats. Journal of Foraminiferal Research 33, 198–218.

Ertekin, I.K., Tunoglu, C., 2008. Pleistocene-Holocene marine ostracods from Mersin offshore sediments, Turkey, eastern Mediterranean. Revue de Micropaléontologie 51, 309–326.

Folk, R.L., Ward, W.C., 1957. Brazos river bar: a study in the significance of grain size parameters. Journal of Sedimentary Petrology 27, 3–26.

Foster, I.D.L., Albon, A.J., Bardell, K.M., Fletcher, J.L., Jardine, T.C., 1991. High energy coastal sedimentary deposits; an evaluation of depositional processes in Southwest England. Earth Surface Processes and Landforms 16, 341–356.

Frenzel, P., Boomer, I., 2005. The use of ostracods from marginal marine, brackish waters as bioindicators of modern and quaternary environmental change. Palaeogeography, Palaeoclimatology, Palaeoecology 225, 68–92.

Fujiwara, O., Masuda, F., Sakai, T., Irizuki, T., Fuse, K., 2000. Tsunami deposits in Holocene bay mud in southern Kanto region Pacific coast of central Japan. Sedimentary Geology 135, 219–230.

Goff, J., McFadgen, B.G., Chagué-Goff, C., 2004. Sedimentary differences between the 2002 Easter storm and the 15th century Okoropunga tsunami, southeastern north island, New Zealand. Marine Geology 204, 235–250.

Grelois, J.-P., 2007. Pierre Gilles, Itinéraires Byzantins. De la topographie de Constantinople et de ses antiquités. Collège de France – CNRS. Centre de recherche, d'histoire et civilisation de Byzance, Monographies 28. Librairie AACHCByz, Paris. 512.

Guernet, C., Lemeille, F., Sorel, D., Bourdillon, C., Berge, T., Manakou, M., 2003. Les ostracodes et le quaternaire d'Aigion (Golfe de Corinthe, Grèce). Revue de micropaléontologie 46, 73–93.

Guidoboni, E., Cosmatri, A., Traina, G., 1994. Catalogue of Ancient Earthquakes in the Mediterranean Area up to the 10th Century. Istituto Nazionale di Geofisica. 504.

Hawkes, A.D., Bird, M., Cowie, S., Grundy-Warr, C., Horton, B.P., Tan Shau Hwai, A., Law, L., MacGregor, C., Nott, J., Eong Ong, J., Rigg, J., Robinson, R., TanMullins, M., Tiong Sa, T., Yasin, Z., Wan Aik, L., 2007. Sediments deposited by the 2004 Indian Ocean tsunami along the Malaysia–Thailand Peninsula. Marine Geology 242, 169–190.

Hébert, H., Schindelé, F., Altınok, Y., Alpar, B., Gazioglu, C., 2005. Tsunami hazard in the Marmara Sea (Turkey): a numerical approach to discuss active faulting and impact on the Istanbul coastal areas. Marine Geology 215, 23–43.

Hussain, S.M., Krishnamurthy, R., Suresh Gandhi, M., Ilayaraja, K., Ganesan, P., Mohan, S.P., 2006. Micropalaeontological investigations on tsunamigenic sediments of Andaman Islands. Current Science 91, 1655–1667.

Kaminski, M.A., Aksu, A., Box, M., Hiscott, R.N., Filipescu, S., Al-Salameen, M., 2002. Late Glacial to Holocene benthic foraminifera in the Marmara Sea: implications for Black sea-Mediterranean Sea connections following the last deglaciation. Marine Geology 190, 165–202.

Kızıltan, Z., 2007. Marmaray Projesi ve İstanbul'un "gün ışığına çıkan" 8000 yılı. In: Gün Işığında İstanbul'un 8000 Yılı. Marmaray, Metro ve Sultanahmet Kazıları. Vehbi Koç Vakfı- İstanbul Arkeoloji Müzeleri, İstanbul, pp. 18–22 (in Turkish).

Kocabaş, U., Özsait-Kocabaş, I., 2009. De Bysance à Istanbul–un port à deux continents. Galeries nationales (Grand Palais, Champs-Elysées). Editions de la Réunion des Musées Nationaux, Paris. 362.

Kortekass, S., Dawson, A.G., 2007. Distinguish tsunami and storm deposits: an example from Martinhal, SW Portugal. Sedimentary Geology 200, 208–221.

Leroy, S., Kazanci, N., Ileri, Ö, Kibar, M., Emre, O., McGee, E., Griffiths, H.I., 2002. Abrupt environmental changes within a late Holocene lacustrine sequence south of the Marmara Sea (Lake Manyas, N-W Turkey): possible links with seismic events. Marine Geology 190, 531–552.

Mango, C., 2001. The shoreline of Constantinople in the Fourth century. In: Necipoglu, N. (Ed.), Byzantine, Constantinople: Monuments, Topography and Everyday Life, vol. 33. The Medieval Mediterranean 17–28.

Mamo, B., Strotz, L., Doniney-Howes, D., 2009. Tsunami sediments and their fora-miniferal assemblages. Earth-Science Reviews 96, 263–278.

Marriner, N., Morhange, C., 2007. Geoscience of ancient Mediterranean Harbours. Earth-Science Reviews 80, 137–194.

Mischke, S., Shudack, U., Bertrand, S., Leroy, S.A.G., 2010. Ostracods from a Marmara Sea lagoon (Turkey) as tsunami indicators. Quaternary International. doi:10.1016/j.quaint.2010.11.013.

Morales, J.A., Borrego, J., San Miguel, E.G., Lopez-Gonzalez, N., Carro, B., 2008. Sedimentary record of recent tsunami in the Huelva Estuary (Southwestern Spain). Quaternary Science Reviews 27, 734–746.

Morhange, C., Marriner, N., 2010. Palaeo-hazards in the coastal Mediterranean: a geoarchaeological approach. In: Martini, I.P., Chesworth, W. (Eds.), Landscapes and Societies. Springer, Berlin 223–234.

Morton, R.A., Gelfenbaum, G., Jaffe, B.E., 2007. Physical criteria for distinguishing sandy tsunami and storm deposits using modern examples. Sedimentary Geology 200, 184–207.

Müller-Wiener, W., 1998. Bizans'tan Osmanlı'ya Istanbul Limanı (Erol Özbek, Trans.), vol. 66. Tarih Vakfı-Yurt Yayınları, Istanbul.

Mundell-Mango, M., 2000. The Commercial Map of Constantinople Dumbarton Oaks Paper 54, 179–207.

Murray, J., 2006. Ecology and Applications of Benthic Foraminifera. Cambridge University Press. 440.

Nachite, D., Rodriguez-Lazaro, J., Martin-Rubio, M., Pascual, A., Bekkali, R., 2010. Distribution et écologie des associations d'ostracodes récents de l'estuaire de Tahadart (Maroc Nord-Occidental). Revue de micropaléontologie 53, 3–15.

Nanayama, F., Shigeno, K., 2006. Inflow and outflow facies from the 1993 tsunami in southwest Hokkaido. Sedimentary Geology 187, 139–158.

Nanayama, F., Shigeno, K., Satake, K., Shimokawa, K., Koitabashi, S., Miyasaka, S., Ishii, M., 2000. Sedimentary differences between the 1993 Hokkaido-nansei-oki tsunami and the 1959 Miyakojima typhoon at Taisei, southwestern Hokkaido, northern Japan. Sedimentary Geology 135, 255–264.

Nazik, A., 2001. Ostracode faunas of bottom sediments from the continental shelf, south Marmara Sea, NW Turkey, and their comparison with other shelf envi-ronments in the Mediterranean and Aegean regions. Geological Journal 36, 111–123.

Papadopoulos, A.G., Fokaefs, A., 2005. Strong tsunami in the Mediterranean Sea: a re-evaluation. ISET Journal of Earthquake Technology 42 (4), 159–170.

Péres, J.M., Picard, J., 1964. Nouveau manuel de bionomie benthique de la mer Méd-iterranée. Recueil des Travaux de la Station marine d'Endoume 31 (47), 137.

Perinçek, D., 1991. Possible strand of the north Anatolian fault, Turkey - An inter-pretation. American Association of Petroleum Geologists Bulletin 75 (2), 241–257.

Perinçek, D., 2008. Geoarchaeology of the Excavation Site for the last 8000 Years and Traces of Natural Catastrophes in Geological Profiles, Istanbul Archaeo-logical Museum. Proceeding of the 1st Symposium on Marmaray-Metro Salvage Excavations 5th–6th May 2008, Turkey, 191–217. (in English and in Turkish).

Perinçek, D., 2010. Yenikapı kazı alanının son 8000 yıllık jeoarkeolojisi ve doğal afetlerin jeolojik kesitteki izleri. The Geoarchaeology of the Yenikapı Excavation Site in the Last 8000 years and Geological Traces of Natural Disasters (İstanbul − Turkey), 141. General Directorate of Mineral Research and Exploration Journal (MTA Dergisi), Ankara, Turkey (in Turkish with English abstract), 73–95.

Perinçek, D., Meriç, E., Pulak, C., Körpe, R., Yalçıner, A.C., Gökçay, M., Kozanlı, C., Avşar, N., Nazik, A., Yeşilyurt, S.K., Gökgöz, Z., 2007. Yenikapı Antik Liman Kazılarında Jeoarkeoloji Çalışmaları ve Yeni Bulgular. Türkiye Jeoloji Kurultayı. Bildiri özetleri Kitabı 131–135, 16–22. Nisan 2007, Ankara (in Turkish).

Poppe, T.G., Goto, Y., 2000a. European Seashells, vol. I. Verlag Christia Hemmen. 352.

Poppe, T.G., Goto, Y., 2000b. European Seashells, vol. II. Conchbooks, 221.

Redois, F., Debenay, J.P., 1996. Influence du continent sur la répartition des fora-minifèresbenthiques, exemple de l'estran d'une ria mésotidale de Bretagne méridional. Revue de Paléobiologie 15, 243–260.

Reimer, P.J., Baillie, M.G.L., Bard, E., Bayliss, A., Beck, J.W., Blackwell, P.G., Bronk Ramsey, C., Buck, C.E., Burr, G.S., Edwards, R.L., Friedrich, M., Grootes, P.M., Guilderson, T.P., Hajdas, I., Heaton, T.J., Hogg, A.G., Hughen, K.A., Kaiser, K.F., Kromer, B., McCormac, F.G., Manning, S.W., Reimer, R.W., Richards, D.A., Southon, J.R., Talamo, S., Turney, C.S.M., Van der Plicht, J., Weyhenmeyer, C.E., 2009. IntCal09 and Marine09 radiocarbon age calibration curves, 0–50,000 years cal BP. Radiocarbon 51 (4), 1111–1150.

Ruiz, F., Abad, M., Caceres, L.M., Vidal, J.R., Carretero, M.I., Pozo, M., Gonzalez-Regalado, M.L., 2009. Ostracods as tsunami tracers in Holocene sequences. Quaternary Research 73, 130–135.

Ruiz-Munoz, F., Gonzalez-Regalado Montero, M.L., Morales Gonzalez, J.A., 1996. Distribucion y Ecologia de los Foraminiferos y Ostracodos actuales del Estuario Mesomareal del Rio Guadiana (SO Espana). Geobios 29 (5), 513–528.

Sağlam, M., Sulukan, E., Uyar, T.S., 2010. Wave energy and technical potential of Turkey. Journal of Naval Science and Engineering 6 (2), 34–50.

Şengör, A.M.C., Görür, N., Şaroglu, F., 1985. Strike-slip Faulting and Related Basin Formation in Zones of Tectonic Escape: Turkey as a Case Study, vol. 37. SEPM Special Publication. 227–264.

Shanmugan, G., 2006. The tsunamite problem. Journal of Sedimentary Research 76, 718–730.

Siani, G., Paterne, M., Arnold, M., Bard, E., Métivier, B., Tisnerat, N., Bassinot, F., 2000. Radiocarbon reservoir ages in the Mediterranean Sea and Black sea. Radio-carbon 42, 271–280.

Siani, G., Paterne, M., Michel, E., Sulpizio, R., Sbrana, A., Arnold, M., Haddad, G., 2001. Mediterranean Sea surface radiocarbon reservoir age changes since the Last Glacial Maximum. Science 294, 1917–1920.

Smith, D.E., Shi, S., Cullingford, R.A., Dawson, A.G., Dawson, S., Firth, C.R., Foster, I.D.L., Fretweel, P.T., Haggart, B.A., Holloway, L.K., Long, D., 2004. The Holocene Storegga slide tsunami in the United Kingdom. Quaternary Science Reviews 23, 2291–2321.

Soloviev, S.L., 1990. Tsunamigenic Zones in the Mediterranean sea. Natural Hazards 3, 183–202.

Soloviev, S.L., Solovieva, O.N., Go, C.N., Kim, K.S., Shchetnikov, N.A., 2000. Tsunami in the Mediterranean Sea 2000 B.C.–2000 A.D. In: Advances in Natural and Technological Hazards Research, vol. 13, 237.

Stiros, S.C., 2010. The 8.5+ magnitude, AD 365 earthquake in Crete: coastal uplift, topography changes, archaeological and historical signature. Quaternary International 216, 54–63.

Tinti, S., Armigliato, A., Manucci, A., Pagnoni, G., Zaniboni, F., Yalçıner, A.Y., Altınok, Y., 2006. The generating mechanism of the August 17, 1999 Izmit bay (Turkey) tsunami: Regional (tectonic) and local (mass instabilities) causes. Marine Geology 225, 311–330.

Tunoglu, C., 2001. Pontian aged Loxoconcha (Ostracoda) species from eastern Black Sea region of Turkey. Yerbilimleri 24, 127–142.

Tuttle, M.P., Ruffman, A., Anderson, T., Jeter, H., 2004. Distinguish tsunami from storm deposits in eastern North America. The 1929 Grand Banks tsunami versus the 1991 Halloween storm. Seismological Research Letters 75, 117–131.

Vött, A., Brückner, H., Brockmüller, S., May, S.M., Gaki-Papanastassiou, K., Herd, R., lang, F., Maroukian, H., Nelle, O., Papalastassiou, D., 2009. Traces of Holocene tsunami across the sound of lefkada, NW Greece. Global and Planetary Change 66, 112–128.

Wassmer, P., Baumert, P., Lavigne, F., Paris, R., Sartohadi, J., 2007. Faciès et transfert sédimentaires associés au tsunami du 26 décembre 2004 sur le littoral au nord-est de Banda Aceh (Sumatra, Indonésie). Géomorphologie: Relief, Processus, Environnement 4, 335–346.

Ward, S.N., 2002. Tsunami. In: Meyers, R.A. (Ed.), The Encyclopedia of Physical Science and Technology, vol. 17. Academic Press, New York, 175–191.

Watson, D.I., O'Riordan, R.M., Barnes, D.K.A., Cross, T., 2005. Temporal and spatial variability in the recruitment of barnacles and the local dominance of Elminius modestus Darwin in SW Ireland. Estuarine, Coastal and Shelf Science 63, 119–131.

Wazny, T., Kuniholm, P., Griggs, C., Perinçek, D., 2010. Trade, earthquakes and tsunami − tree-ring study on Yenikapı harbor in Istanbul. In: Mielikäinen, K., Mäkinen, H., Timonen, M. (Eds.), World Dendro, the 8th International Confer-ence on Dendrochronology, Abstract, 194.

Yalçıner, A.C., Alpar, B., Altınok, Y., Özbay, I., Imamura, F., 2002. Tsunami in the Sea of Marmara Historical documents for the past, models for the future. Marine Geology 190, 445–463.

Yaltırak, C., Alpar, B., 2002. Kinematics and evolution of the northern branch of the north Anatolian fault (Ganos fault) between the Sea of Marmara and the Gulf of Saros. Marine Geology 190, 351–366.

Yaltırak, C., 2002. Tectonic evolution of the Marmara Sea and its surroundings. Marine Geology 190, 493–529.